

# The Equilibrium Photoionized Absorber in 3C351

Fabrizio Nicastro<sup>1,2</sup>, Fabrizio Fiore<sup>1,2,3</sup>, G. Cesare Perola<sup>4</sup>, Martin Elvis<sup>1</sup>

<sup>1</sup> Harvard-Smithsonian Center for Astrophysics

60 Garden St, Cambridge MA 02138

<sup>2</sup> Osservatorio Astronomico di Roma

via Osservatorio, Monteporzio-Catone (RM), I00040 Italy

<sup>3</sup> SAX Science Data Center

via Corcolle 19, Roma I00100 Italy

<sup>4</sup> Dipartimento di Fisica, Università degli studi "Roma Tre"

Via della Vasca Navale 84, Roma, I00146 Italy

version: 18:00, 8 August, 1998

## ABSTRACT

We present two ROSAT PSPC observations of the radio-loud, lobe-dominated quasar 3C 351, which shows an 'ionized absorber' in its X-ray spectrum. The factor 1.7 change in flux in the  $\sim 2$  years between the observations allows a test of models for this ionized absorber.

The absorption feature at  $\sim 0.7$  keV (quasar frame) is present in both spectra but with a lower optical depth when the source intensity - and hence the ionizing flux at the absorber - is higher, in accordance with a simple, single-zone, equilibrium photoionization model. Detailed modeling confirms this agreement quantitatively. The maximum response time of 2 years allows us to limit the gas density:  $n_e > 2 \times 10^4 \text{ cm}^{-3}$ ; and the distance of the ionized gas from the central source  $R < 19$  pc. This produces a strong test for a photoionized absorber in 3C 351: a factor 2 flux change in  $\sim 1$  week in this source *must* show non-equilibrium effects in the ionized absorber.

## 1. INTRODUCTION

The most luminous known AGN with an ionized absorber is the radio-loud lobe-dominated <sup>1</sup> quasar 3C351 ( $L_{0.1-2keV} = 2.3 \times 10^{45}$  erg s<sup>-1</sup>,  $z=0.371$ , Fiore et al., 1993). Ionized absorbers are common in low redshift, low luminosity Seyfert 1 galaxies (Reynolds, 1997), but rare in higher redshift, higher luminosity quasars. High luminosity AGNs are very likely physically larger and so may exhibit slower time variability and have different physical conditions. 3C 351 has a very high UV to X-ray ratio ( $\alpha_{OX} = 1.55$ , Tanambaun et al., 1989) and its IR to UV spectrum does not show any evidence of reddening, in contrast to several low redshift Seyfert 1 galaxies thought to host dusty/warm absorbers <sup>2</sup>. Only two other radio-loud quasars, 3C 212 (Mathur et al., 1994) and 3C 273 (Grandi et al, 1997), have candidate ionized absorbers.

The main absorption feature in the ROSAT PSPC X-ray spectrum of 3C 351 is a deep edge at  $\sim 0.7$  keV (quasar frame), which is likely to be due to OVII-OVIII. Mathur et al. (1994) built a simple one-zone model of this absorber that also explained the OVI, CIV and Ly $\alpha$  UV absorption lines seen in a nearly simultaneous HST FOS spectrum. Such simple models, although elegant, have come under criticism. Ionized absorbers in some Seyfert galaxies show different variability behavior in different absorption features, some of which are not as predicted for gas in photoionization equilibrium. Multiple absorbing zones have been introduced to explain these effects (e.g. Reynolds 1997). In another paper (Nicastro et al., 1998) we instead explore additional physics (non-equilibrium photoionization models and collisional models) while retaining a single zone of absorbing gas. 3C 351 is a relatively slowly varying source, compared to the rapidly variable Seyfert with warm absorbers. This persistent variability on timescales that span possible ionization and recombination times makes it hard to define an initial equilibrium state. In contrast 3C 351 presents a simplified situation in which to study changes in the ionization state in response to luminosity changes. Here we show that in 3C 351 at least the simplest photoionization equilibrium, single zone model continues to be sufficient.

3C351 was observed twice by ROSAT, on 1991 October and 1993 August. The first observation was reported by Fiore et al. (1993). The second observation was then proposed in order to search for time variability that could test photoionization models. Fortunately a factor 1.7 decrease in the PSPC count rate was seen, providing just such a test. Here we present the second data set and compare the results with predictions.

---

<sup>1</sup>only 0.65 % of the flux density is contained in the compact core at 6 cm, (Kellerman et al., 1989).

<sup>2</sup>i.e. IRAS 13349+2438, Brandt et al., 1996, 1997; IRAS 17020+4544, Leighly et al., 1997, Komossa & Bade, 1998; MCG-6-30-15, Reynolds et al., 1997.

## 2. Observations and Data Analysis

We considered the two PSPC observations of 3C351 taken roughly two years apart, in 1991 October and 1993 August. Table 1 gives, for each observation, the observation date, its duration, the net exposure time, the net source counts, the count rate, and the signal to noise ratio. The data reduction and the timing analysis were performed using XSELECT.

We reduced the second PSPC observation of 3C351 following the procedures used in Fiore et al. (1993) for the first observation. For the first observation we used the spectrum and light curve obtained by Fiore et al. (1993). The source intensity was consistent with a constant value during both PSPC observations, with no more than 20% change in the  $\sim 2$  day and  $\sim 13$  day spans of the two observations. 3C 351 thus appears more stable than the lower luminosity seyferts with ionized absorber (Reynolds, 1997). Since 3C 351 has a flat X-ray spectrum and broad optical emission lines it is consistent with the trend exhibited by the three similar but radio-quiet, PG quasars of the Fiore et al. (1998) sample. Those quasars show little or no variability on timescales as short as 10 days (compared to the narrow line objects of that sample which are rapidly variable and have steep X-ray spectra). However the mean count rate dropped by a factor  $\sim 1.7$  during the 22 months between the observations (see Table 1), again consistently with the Fiore et al. (1998) discovery. Hereinafter we shall call these the 'High' and 'Low' states, respectively.

## 3. Ionization Models

We produced equilibrium photoionization models and pure collisional ionization models using CLOUDY (version 90.01, Ferland 1996) to fit to the PSPC spectra of 3C 351. We use a Friedman cosmology with  $H_0 = 50 \text{ km s}^{-1} \text{ Mpc}^{-1}$  and  $q_0 = 0.1$  to derive a luminosity of  $L_{2keV} \sim 3 \times 10^{44} \text{ erg s}^{-1} \text{ keV}^{-1}$  for the quasar. This determines the distance scale in the absorber for a given value of the ionization parameter, U.

3C 351 is a radio-loud lobe-dominated quasar and, as Fiore et al (1993) and Mathur et

Table 1: ROSAT PSPC observations of 3C 351

Start Date	Duration (ksec)	Exposure (ksec)	Net Counts	Count Rate ct s <sup>-1</sup>	S/N	State	ROR
91 Oct 28	168	13.1	1390	0.110	31.0	High	rp700439
93 Aug 23	1143	15.4	980	0.064	26.0	Low	rp701439

al (1994) have shown, the ionization state of the gas strongly depends on the spectral energy distribution (SED) of the ionizing continuum, from radio to hard X-rays. We therefore made our photoionization models using the observed SEDs for 3C351 (Mathur et al 1994). We varied the ill-determined energy at which the X-ray spectrum turns up to meet the ultraviolet using a broken power-law with a break energy from the unobserved EUV range to well within or above the PSPC range, as in Mathur et al (1994). The low energy spectral index is fixed by the observed flux in the UV at one end, and the break energy at the other. The high energy spectral index above the break energy is fixed at  $\alpha_E = 0.9$ . This is typical for lobe dominated radio loud quasars (Shastri et al., 1993). In the following we present a spectral analysis using a photoionizing continuum with a break energy of 0.4 keV (quasar frame) and UV-to-soft-X-ray index of  $\alpha_E = 1.5$ . We note however that this continuum model, although providing a good description of the PSPC data, should only be thought as one of the possible continuum parameterization connecting the UV and the soft X-ray data of 3C 351. No break energy is required by data, which are well fitted by a simple power law with  $\alpha_E = 0.9$  across the whole PSPC band.

### 3.1. Spectral Analysis

The spectral analysis was performed using XSPEC and the latest version of the 256 channels PSPC response matrix (“pspcb\_gain2\_256.rsp”, released on January 12, 1993). We binned each spectrum in channels with at least 50 counts, to warrant the poissonian statistics to be used.

We first fitted the high and low state spectra with a simple power law model reduced at low energy by Galactic absorption ( $2.26 \times 10^{20} \text{ cm}^{-2}$ , Elvis et al., 1989). Only 2 parameters were left free to vary: the photon spectral index  $\Gamma$  and the normalization  $F_0$ . In both the cases the  $\chi^2$  is unacceptably high:  $\chi_r^2 = 2.99$  and  $3.09$ , for 46 and 19 degree of freedom respectively. The upper panels of Fig. 1 (a) and (b), show the data and the best fit simple power law models folded with the PSPC response, for the High and Low state respectively ( $\alpha_E^{High} = 1.3$  and  $\alpha_E^{Low} = 1.0$ ). Lower panels show the ratio between the data and the best fit models. The deficit of counts at  $\sim 0.6$  keV (rest frame) is evident in both spectra. We tested more complex models for the intrinsic continuum, adding a second power law, and a low energy black body component. In the latter case the  $\chi^2$  was still unacceptably high, while a double power law, though producing acceptable fits by the  $\chi^2$  point of view, gave uncommon spectral index values for this class of sources. Furthermore in both the cases negative residuals were still evident around 0.6 keV (observed). Following Fiore et al. (1993) we then interpret these features as due to a blend of OVII-OVIII absorption K-edges

caused by ionized gas along the line of sight. A test of this by making a fit of a single power law with a notch at 0.6 keV (observed) – a simplistic ionized absorber model – gave acceptable  $\chi^2$ : 1.1 (45 dof) and 1.0 (18 dof) for the High and the Low state respectively.

We then fitted both spectra using the equilibrium photoionization models described above. Only three parameters were left free to vary in the fit: the normalization ( $F_0$ ), the ionization parameter  $U = \left( \int_{1R_{yd}}^{+\infty} F_E dE \right) / (4\pi R^2 n_e c)$  and the warm absorber column density  $N_H$ . The soft ( $E < 0.29$  keV) and hard ( $0.29 < E < 2.5$  keV) spectral index were fixed at  $\alpha_E^{UV-X} = 1.4$  and  $\alpha_E = 0.9$ , the values of the ionizing continuum used to build the models (see above). Table 2 gives the best fit parameters. While the best fit values of  $N_H$  are consistent with a constant value, there is marginal evidence (at the  $2\sigma$  level) of variation in  $U$ .

We then fitted the high and low state spectra simultaneously, fixing  $N_H$  to the best fit value found in the high state, since this has the best statistics. Table 2 gives again the best fit values for  $U$  and the  $F_0$  in the two spectra (with the 90% confidence intervals for one interesting parameter). The best fit  $U$  and  $F_0$  are linearly correlated with each other (Figure 2), in the manner expected if the gas is in photoionization equilibrium with the ionizing continuum. Table 2 also gives the best fit abundances of OVII and OVIII and their ratio. The change of  $U$  translates to a factor of three change in the OVII to OVIII ratio as the source intensity drops by about 70 %.

Collisional ionization models can fit the data equally well, as they should at low column densities (Nicastrò et al., 1997). To do so however they require arbitrary changes, by a factor 1.5 in temperature or a factor 2 in  $N_H$ . Instead photoionization equilibrium models predict the observed correlation with the ionizing continuum. To the authors this is a strong argument in favor of a photoionization model.

Table 2: **Equilibrium Photoionization Model Fits**

Spectrum	$\text{Log}(N_H)$	$\text{Log}(U)$	${}^a F_0$	$\chi^2(\text{d.o.f.})$	$n_{OVIII}$	$n_{OVIII}$	$n_{OVIII}/n_{OVII}$
High	$22.14^{+0.14}_{-0.17}$	$0.78^{+0.21}_{-0.13}$	$8.9 \pm 1.8$	0.89(45)	0.783	0.168	0.03
Low	$21.89^{+0.22}_{-0.28}$	$0.49^{+0.23}_{-0.30}$	$5.0 \pm 0.1$	0.89(18)	0.822	0.081	0.10
High+Low	22.14 (frozen)	$0.78^{+0.12}_{-0.09}, 0.63^{+0.10}_{-0.09}$	$8.7^{+0.9}_{-0.8}, 6.0^{+0.7}_{-0.5}$	0.99(62)			

<sup>a</sup> in  $10^{-5}$  ph s<sup>-1</sup> cm<sup>-2</sup> keV<sup>-1</sup> (at 1 keV).

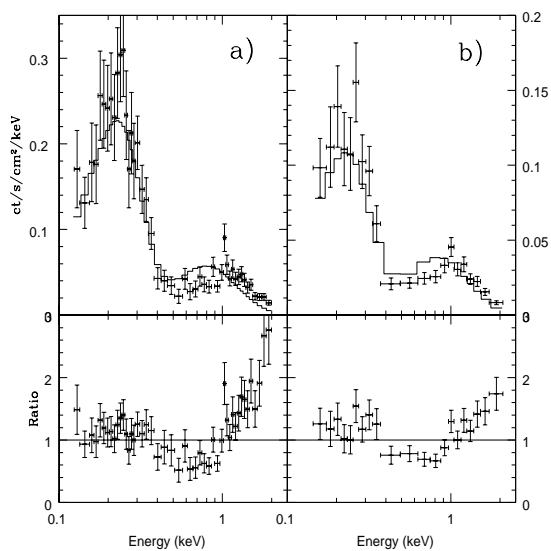


Fig. 1.— High and low state PSPC spectra of 3C 351 along with the best fit simple power law models folded with the PSPC response (Fig. 1a and 1b respectively, upper panels). Ratio between the data and the best fit models (lower panels).

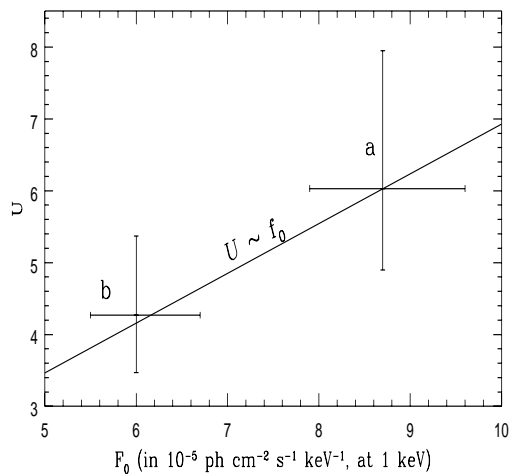


Fig. 2.— Best fit ionization parameter  $U$  versus best fit 1 keV normalizations  $F_0$  for spectra 'High' and 'Low'. The solid line shows the linear relationship  $U(F_0)$  expected if photoionization equilibrium applies.

### 3.2. X-ray Colors of the warm absorbers in 3C 351

The behavior of the main physical properties of the absorber can be seen in a color-color diagram. In Fig. 3 we plot the hardness ratios  $HR=H/M$  against the softness ratio  $SR=S/M$  from the count rates in three bands ( $S=0.15-0.58$  keV,  $M=0.88-1.47$  keV, and  $H=1.69-3.40$  keV, at  $z=0.371$ ) for theoretical curves (for  $\log(N_H)=21, 21.5, 22$  and  $22.14$ ) obtained by folding the equilibrium photoionization models (for  $\log(U)$  in the range  $-0.3-1.5$ , and Galactic  $N_H$ ) with the response matrix of the PSPC.

The position of a point in this diagram readily gives the dominant ion in the gas. The rapid change of  $SR$  as  $U$  increase from 0.5 to 5.5 (on the curve corresponding to  $\log(N_H)=22.14$ ) corresponds to large increases of the transparency of the gas at  $E < 0.5$  keV as H and He becomes rapidly fully ionized. As  $U$  further increases from 5.5 to 16.5 the  $SR$  color changes more slowly, and inverts its trend at  $U \sim 11$ , with  $HR$  now changing more rapidly than  $SR$ . The inversion point indicates the switch from an ionization state dominated by OVII to that dominated by OIX. In the last part of the curve as  $U$  increases,  $SR$  and  $HR$  decrease until all the ions in the gas are fully stripped and the gas is completely transparent to radiation of any energy.

The two data points show the two 3C 351 observations. The best fit  $U$  in the High observation is marked on the  $\log(N_H)=22.14$  curve along with the value obtained by scaling by the intensity ratio between the two observations (a factor 1.7). The two points are consistent with the position of the observed colors of 3C351 in the two observations, so the predictions of the simple equilibrium photoionization model is consistent with the data.

## 4. Discussion

The as predicted change of the ionization parameter in the 3C 351 absorber to a change in the ionizing continuum is strong evidence that photoionization is the dominant ionization mechanism. We also see that the absorber comes to ionization equilibrium within 22 months, and can use this to constrain the physical properties of the absorber.

The time  $t_{eq}$  measures the time the gas needs to reach equilibrium with the instantaneous ionizing flux (Nicastro et al, 1997). This time depends on the particular ionic species considered. The ionic abundances of Oxygen in the absorber in 3C 351 are distributed mainly between only two ionic species: OVII and OVIII. In this simple case a useful analytical approximation for  $t_{eq}$  is:

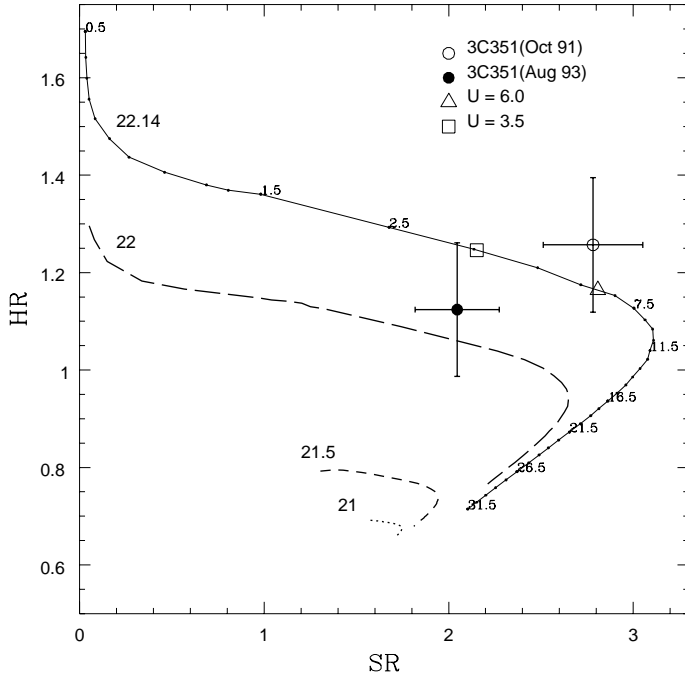


Fig. 3.— Color-color diagram of the two observations of 3C351. Lines are theoretical photoionization curves, built folding equilibrium photoionization models with the response matrix of the PSPC. Different lines correspond to two different values of the gas column density:  $\log(N_H)=22.14$  (solid line),  $\log(N_H)=22$  (dashed line). On each curve the ionization parameter  $U$  increases going from top to bottom.  $U$  values are indicated on the  $\log(N_H)=22.14$  line. On the same curve we mark two points: a) the best fit  $U$  to the october 1991 observation, and b) this value scaled by the factor 1.7 (the ratio of the source fluxes).



$$t_{eq}^{OVII,OVIII}(t \rightarrow t + \Delta t) \sim \frac{1}{\alpha_{rec}(OVII, T_e)_{eq} n_e} \frac{1}{\left[ \left( \frac{\alpha_{rec}(OVI, T_e)}{\alpha_{rec}(OVII, T_e)} \right)_{eq} + \left( \frac{n_{OVIII}}{n_{OVII}} \right)_{eq} \right]_{t+\Delta t}}$$

where  $eq$  indicates the equilibrium quantities.

By requiring that  $t_{eq}$  for OVII and OVIII species is shorter than the  $4.2 \times 10^7$  s (quasar frame) elapsed between the two observations, we can find a lower limit to the electron density of the absorber:  $n_e > 2.5 \times 10^3 \text{ cm}^{-3}$ . Since we know the values of  $U$  and  $F_0$ , this density limit translates into a limit on the distance of the ionized gas from the central source,  $R < 50 \text{ pc}$ .

These limits are consistent with the upper limit of  $n_e < 5 \times 10^7 \text{ cm}^{-3}$ , and  $R > 0.3 \text{ pc}$ , found by Mathur et al. (1994) using a lower limit for the distance of the cloud from the central source, based on the absorber being outside the broad emission line region.

The relative closeness of these two limits (factor  $\sim 100$ ) implies that a variation in shorter times ( $\sim 1$  month), would be likely to show non-equilibrium effects (Nicastro et al, 1997). If a factor 2 flux change in  $\lesssim 1$  week showed no such effects the simplest photoionization model would have to be abandoned.

## 5. Conclusion

We have tested ionization models for the ionized absorber in 3C 351. In particular, we tested a simple one zone photoionization equilibrium model on two PSPC spectra of 3C 351 that show a factor  $\sim 2$  decrease in flux. The model correctly predicts the sense and amplitude of the observed change in the ionization state of the absorber, correlated with the ionizing continuum flux.

Given that photoionization equilibrium applies we can derive a lower limit to the electron density of the absorber:  $n_e > 2.5 \times 10^3 \text{ cm}^{-3}$ . This is consistent with the upper limit of  $n_e < 5 \times 10^7 \text{ cm}^{-3}$  found by Mathur et al. (1994). The distance of the ionized gas from the central source is then  $0.3 \text{ pc} < R < 50 \text{ pc}$ . The closeness of these two limits creates a strong test of photoionization models: factor 2 variations in 3C 351 on timescales of order a week *must* show non-equilibrium effects.

## Acknowledgements

This work was supported in part by NASA grants NAG5-3066 (ADP), NAG5-2640 (ROSAT), NAGW-2201 (LTSA)

## REFERENCES

- Brandt W.N., Fabian A.C., Pounds K.A., 1996, MNRAS, 278, 326
- Brandt W.N., Mathur S., Reynolds C.S., Elvis M., 1997, MNRAS, 292, 407
- Elvis M., Wilkes B.J., Lockman F.J., 1989, A.J., 97, 777
- Ferland G.J., 1996, CLOUDY: 9001
- Fiore F., Elvis M., Mathur S., Wilkes B.J., McDowell J.C. 1993, ApJ, 415, 192
- Grandi P., et al., 1997, A&A, 325, 17
- Kellerman K.I., Sramek R., Schmidt M., Shaffer D.B., & Green R., 1989, AJ, 98, 1195
- Komossa S. & Bade N., 1998, A&A, 331, 49
- Leighly K.M., Kay L.E., Wills B.J., Wills D., & Grupe D., 1997, ApJL, 489, 137
- Mathur S., 1994, ApJ, 431, 75
- Mathur S., Wilkes B.J., Elvis M., Fiore F. 1994, ApJ, 434, 493
- Nicastro F., Fiore F., Perola G.C., Elvis M., 1998, Apj submitted
- Reynolds C.S., 1997, MNRAS, 286, 513
- Reynolds C.S., Ward M.J., Fabian A.C. & Celotti A., 1997, MNRAS, 291, 403
- Shastri P., Wilkes B.J., Elvis M., McDowell J. 1993, ApJ, 410, 29
- Tanambaum H., Avni Y., Green R.F., Schmidt M., & Zamorani G., 1986, ApJ, 305, 57